Hindawi
Advances in Polymer Technology
Volume 2019, Article ID 4375838, 11 pages
https://doi.org/10.1155/2019/4375838

Research Article

Self-Assembly Investigations of Sulfonated Poly(methyl methacrylate-*block*-styrene) Diblock Copolymer Thin Films

Claudia Piñón-Balderrama,[1] **César Leyva-Porras**,[2] **Roberto Olayo-Valles**,[3] **Javier Revilla-Vázquez**,[4] **Ulrich S. Schubert**,[5,6] **Carlos Guerrero-Sanchez**,[5,6] **and José Bonilla-Cruz**[1]

[1]*Advanced Functional Materials & Nanotechnology Group, Polymer Science and Nanotechnology Lab, Centro de Investigación en Materiales Avanzados S.C. (CIMAV-Unidad Monterrey), Av. Alianza Norte # 202, PIIT, Autopista Monterrey-Aeropuerto Km 10, C.P. 66628, Apodaca, NL, Mexico*
[2]*Centro de Investigación en Materiales Avanzados S. C. (CIMAV), Miguel de Cervantes # 120, Complejo Industrial Chihuahua, C.P. 31136, Chihuahua, Chih, Mexico*
[3]*Departamento de Física, Universidad Autónoma Metropolitana-Iztapalapa, Av. San Rafael Atlixco 186, C.P. 09340, Mexico City, Mexico*
[4]*Departamento de Ingeniería y Tecnología, División Ciencias Químicas, Facultad de Estudios Superiores Cuautitlán-UNAM, Av. Primero de Mayo s/n Cuautitlán Izcalli, C.P. 54740, Estado de México, Mexico*
[5]*Laboratory of Organic and Macromolecular Chemistry (IOMC), Friedrich Schiller University Jena, Humboldtstr. 10, 07743 Jena, Germany*
[6]*Jena Center for Soft Matter (JCSM), Friedrich Schiller University Jena, Philosophenweg 7, 07743 Jena, Germany*

Correspondence should be addressed to Carlos Guerrero-Sanchez; carlos.guerrero.sanchez@uni-jena.de and José Bonilla-Cruz; jose.bonilla@cimav.edu.mx

Received 24 October 2018; Revised 8 January 2019; Accepted 18 February 2019; Published 1 April 2019

Academic Editor: Katja Loos

Copyright © 2019 Claudia Piñón-Balderrama et al. This is an open access article distributed under the Creative Commons Attribution License, which permits unrestricted use, distribution, and reproduction in any medium, provided the original work is properly cited.

Poly(methyl methacrylate-*block*-styrene) block copolymers (BCs) of low dispersity were selectively sulfonated on the styrenic segment. Several combinations of degree of polymerization and volume fraction of each block were investigated to access different self-assembled morphologies. Thin films of the sulfonated block copolymers were prepared by spin-coating and exposed to solvent vapor (SVA) or thermal annealing (TA) to reach equilibrium morphologies. Atomic force microscopy (AFM) was employed for characterizing the films, which exhibited a variety of nanometric equilibrium and nonequilibrium morphologies. Highly sulfonated samples revealed the formation of a honeycomb-like morphology obtained in solution rather than by the self-assembly of the BC in the solid state. The described morphologies may be employed in applications such as templates for nanomanufacturing and as cover and binder of catalytic particles in fuel cells.

1. Introduction

Block copolymers (BCs) have become promising materials in applications where well-defined nanostructures are required such as photonic crystals [1], high-density information storage devices [2] or templates for metals [3], and semiconducting nanowires [4]. The ease to prepare complex morphologies with controllable size, shape, and periodicities of domains, positions them as ideal candidates for the aforementioned applications. A wide range of desired morphologies of BCs can be predicted by the mean field theory and summarized in a phase diagram, which typically are defined by the degree of polymerization (N), the volume fraction (ϕ), and the Flory-Huggins interaction parameter (χ). Once χ, N, and ϕ are set, phase separation of BCs can yield arrays of periodic patterns with length scales in the range from 10 to 100 nm, which can be accessed by different treatments such as solvent vapor annealing (SVA) [5], thermal annealing (TA)

[6], or application of an electric field [7]. The Flory-Huggins interaction parameter describes repulsive energies between different polymers and is a measure of the degree of phase separation for a given polymeric combination. Repulsive energies are derived from thermodynamic incompatibility of different polymers, where the larger the chemical difference, the higher and positive the value of χ. Additionally, when the BC is confined to a surface, i.e., in the form of a thin film, there are other experimental parameters that may influence the resulting morphology, and usually these parameters are not included in phase diagram representations. For example, Zhao et al. employed a selective solvent during the SVA treatment of poly(methyl methacrylate-*block*-styrene) (PMMA-*b*-PS) and found that the resulting morphology depended on the swelling ratio of the segments [8]. According to Yang & Loose, for the poly(styrene-*b*-2-vinylpyridine) (PS-*b*-P2VP) system, the obtained morphologies resulted in a perpendicular orientation with respect to the substrate surface only to film thickness of 0.4-0.8L_o [9]. Nehache et al. studied the triblock copolymer system poly(styrene-*b*-styrenesulfonic acid sodium salt-*b*-styrene) (PS-*b*-PSSNa-*b*-PS) dissolved at different compositions of tetrahydrofuran (THF)-water, finding the formation of a porous morphology at low and medium concentrations [10].

The phase separation of poly(methyl methacrylate-*block*-styrene) (PMMA-*b*-PS) BCs has been widely studied since these two blocks have similar surface energies and a relative high χ (i.e., χ = 0.04 at 120°C) [11], which promotes a phase separation between these blocks [12–14]. However, only few contributions in the literature have discussed the self-assembly process of sulfonated PMMA-*b*-PS in bulk or in membranes. For example, Rubatat *et al.* studied the relationship of proton conductivity with morphology of partially sulphonated PMMA-*b*-PS (PMMA-*b*-sPS) BCs in bulk [15]. For this purpose, PMMA-*b*-PS BCs of different molar mass were partially sulfonated with a degree of sulfonation (DS) of 34 % and subjected to solvent vapor annealing (SVA) (THF vapors) and TA, to obtain hexagonal-packed cylinders, hexagonally perforated lamellas, and lamellar structures. Erdogan et al. synthesized two PMMA-*b*-PS BCs with a high PS content (88 and 93 mol %) [16]. These polymers were partially sulfonated (DS<30 %) and subsequently used to prepare physical blends of PMMA-*b*-sPS/ poly(vinylidene fluoride). They observed that the induced phase separation yielded an enhanced proton conductivity of 151 mS cm^{-1} at 100% of relative humidity.

Thus, to the best of our knowledge, there are no investigations of self-assembly morphologies of highly sulfonated PMMA-*b*-sPS BCs (DS >50 %) in thin films, where high levels of DS might induce a more pronounced phase segregation and stronger interactions with the substrate surface. Therefore, in this contribution, several well-defined PMMA-*b*-PS BCs of different block composition, molar mass, and low dispersity were converted to their analogous ionomer materials by means of a selective sulfonation on the PS block at relatively low temperature. Thereafter, self-assembled morphologies in thin films of these PMMA-*b*-sPS BCs were investigated by atomic force microscopy (AFM), and the obtained morphologies were identified after comparing with those reported in literature. The methodology presented in this work is an alternative to access nanostructured materials without further annealing treatment that may be employed even in bulk state as polyelectrolytes or in the form of thin films for covering and binding catalytic particles and providing conductive pathways for ions and reactant species in fuel cell applications.

2. Experimental Section

2.1. Materials. Acetic anhydride (99 %) and sulfuric acid (99.99 %) were purchased from Aldrich. All solvents were analytical grade (Fluka). PMMA macroinitiators ranging from 8.4 to 42.8 kg/mol and dispersity from 1.07 to 1.09 were used for the synthesis of the BCs using 2-cyanoprop-2-yl-dithiobenzoate as chain transfer agent according to the reported information by the supplier. Poly(methyl methacrylate-*block*-styrene) (PMMA-*b*-PS) block copolymers (BCs) of different composition and molar mass and narrow dispersity ($Đ = M_w/M_n$) were kindly donated by Polymer Libraries GmbH (Germany).

2.2. Instrumentation. Proton nuclear magnetic resonance (^{1}H-NMR) spectra were recorded at room temperature on a Bruker AVANCE 400 MHz spectrometer using deuterated chloroform ($CDCl_3$) and deuterium oxide (D_2O) as solvents. Infrared spectra were measured in a high-throughput FT-IR Brucker MTS-XT apparatus with a range from 4000 to 400 cm^{-1} using 32 scans and a resolution of 4 cm^{-1}. The sulfur content in each sample (wt. %) was measured in an inductively coupled plasma (ICP) spectrometer (Thermo Scientific Model iCAP 6500 Series). The morphology of bulk samples was characterized by small-angle X-ray scattering (SAXS). Samples were exposed to solvent vapors of toluene-dioxane (50/50 v%) for 72 h and dried under vacuum before characterization; data were collected at room temperature and atmospheric pressure in a SAXS instrument (Xeuss, Xenocs) equipped with a Cu-Kα source (GeniX3D, Xenocs) and a 2D hybrid detector (Pilatus 300K, Dectris). The sample-detector distance was 1160 mm. The surface characterization of thin films was carried out in an Asylum Research atomic force microscope model MFP3D-SA in tapping mode. The scanning areas were in the range from 2 to 5 μm^2 using a scanning rate of 0.20 to 1.0 Hz and a rectangular cantilever model AC240TS-R3 at 70 kHz of frequency with a nominal spring constant of 2 $N{\cdot}m^{-1}$ and a radius of nominal curvature of 9±2 nm. Film thicknesses were estimated with a F20 thin film advanced spectrometer system using a beam size of 2 mm in diameter, a wavelength in the range from 200 to 1100 nm, a light source of a deuterium-halogen lamp, and the respective refractive index of poly(methyl methacrylate) (PMMA) and PS.

2.3. Sulfonation Procedure of PMMA-b-PS BCs. The PS block in the PMMA-*b*-PS BCs was selectively sulfonated as follows:

Table 1: Macromolecular characteristics and estimated properties of the investigated PMMA-*b*-PS BCs.

ID	PMMA macroinitiator M_n (kg·mol^{-1})/$Đ$	PMMA-*b*-PS M_n (kg·mol^{-1})/$Đ$	w_{PMMA}	ϕ_{PMMA}	χN
M1	8.4 / 1.12	-	-	-	-
M1_76/24	-	10.8 / 1.11	0.778	0.759	4.06
M1_55/45	-	14.6 / 1.14	0.575	0.549	5.44
M2	39.3 / 1.11	-	-		-
M2_56/44	-	66.7 / 1.17	0.589	0.563	24.9
M2_52/48	-	71.2 / 1.15	0.552	0.525	26.5
M3	42.8 / 1.09	-	-		-
M3_60/40	-	68.8 / 1.20	0.622	0.596	25.7
M3_69/31	-	68.1 / 1.27	0.712	0.689	22.5

M_n = Number average molar mass
$Đ$ = polydispersity
w_{PMMA} = mass fraction of the PMMA block
ϕ_{PMMA} = Volume fraction of the PMMA block
$\chi \cdot N$ = Product of the Flory-Huggins interaction parameter and the total degree of polymerization. c was calculated at a temperature of 120°C which is the glass transition temperature of PMMA.

Acetyl sulfate was used as sulfonating agent (SA) and was prepared before each reaction following a modified procedure reported by Weiss and coworkers [17]. First, acetic anhydride was cooled at 0°C followed by the dropwise addition of sulfuric acid, until a molar relationship of 1.75:1 acetic anhydride to sulfuric acid was reached. The SA stoichiometric concentration was calculated according to the molar content of styrenic units present in the PS block. Different DS in the PS block can be obtained by varying the amount of SA utilized during the sulfonation reaction. A general procedure to carry out this reaction is as follows: 3 g of the respective PMMA-*b*-PS was dissolved in 30 mL of dry dichloroethane and placed into individual glass-reactors of a Chemspeed automated parallel synthesizer [18]. The reactors were heated up to 40 °C under an inert gas atmosphere. Once the desired temperature was reached, a predetermined amount of SA was added dropwise using the automated liquid handling system of the synthesizer. The reaction was stopped after 5 h by adding methanol (in excess) to obtain different PMMA-*b*-sPS BCs, which were purified by precipitation into a nonpolar solvent (cold hexane) and redissolved in chloroform (this procedure was repeated three times). The precipitated PMMA-*b*-sPS's were recovered by decanting the excess of solvent and dried under vacuum at room temperature for 48 h prior characterization.

2.4. Preparation of Thin Films of PMMA-b-PS and PMMA-b-sPS BCs. Thin films of PMMA-*b*-PS and PMMA-*b*-sPS BCs were prepared using a spin coating technique. To obtain smooth films with nanometric thickness, polymer solutions of 0.5 to 1.0 (wt. %) were prepared in toluene-dioxane (50/50 vol %) for PMMA-*b*-sPS BCs. In the case of PMMA-*b*-PS BCs only toluene was used as solvent. All polymeric solutions were filtered and then deposited on a silicon wafer (containing a very thin layer of native oxide SiOx of 6 to 10 nm of thickness) and spin-coated at 3000 rpm for 30 s (two cycles). With this procedure, thin films with nanometric thickness were obtained.

3. Results and Discussion

3.1. Selective Sulfonation of PMMA-b-PS BCs. A sulfonation reaction was carried out in the PMMA-*b*-PS BCs to modify the PS aromatic rings with a sulfonic acid group as was described in the experimental part. This reaction follows an electrophilic aromatic substitution mechanism as reported elsewhere [19]. Sulfonation directly proceeds for aromatics, though the dissociation energy of the C-H bond is higher in aromatic (428 kJ/mol) than in aliphatic (374 to 384 kJ/mol) compounds; only one sulfonic acid group (SO_3H) may be attached to the carbon atom of an aromatic ring [20]. Consequently, PMMA-*b*-PS BCs can be selectively sulfonated in the PS block, where the SO_3H groups react with the aromatic rings of the styrenic segments to form *p*-substituted products. Briefly, the sulfonation reaction proceeds in two main steps: the first step corresponds to the addition of the strongly electrophilic sulfonic acid group, which reacts with the delocalized π electron system of an aromatic ring. In the second reaction step, a hydrogen atom is abstracted by an oxygen atom (anion, produced in the first step) and produces acetic acid as a byproduct. This reaction will be further discussed in more detail based on ^{1}H-NMR analysis. Table 1 summarizes the macromolecular characteristics of the utilized PMMA-*b*-PS BCs as well as other properties estimated herein. As reported by the supplier, PMMA-*b*-PS BCs were prepared by reversible addition-fragmentation chain transfer (RAFT) polymerization. The volume fraction of the PMMA block (ϕ_{PMMA}) was estimated assuming the additivity of volume and using the densities of PS (ρ_{PS} = 1.05 g cm^{-3}) and PMMA (ρ_{PMMA} = 1.17 g cm^{-3}) at room temperature [15]. The $Đ$ of the polymers is relatively low, which is an indication of well-defined BCs. Furthermore,

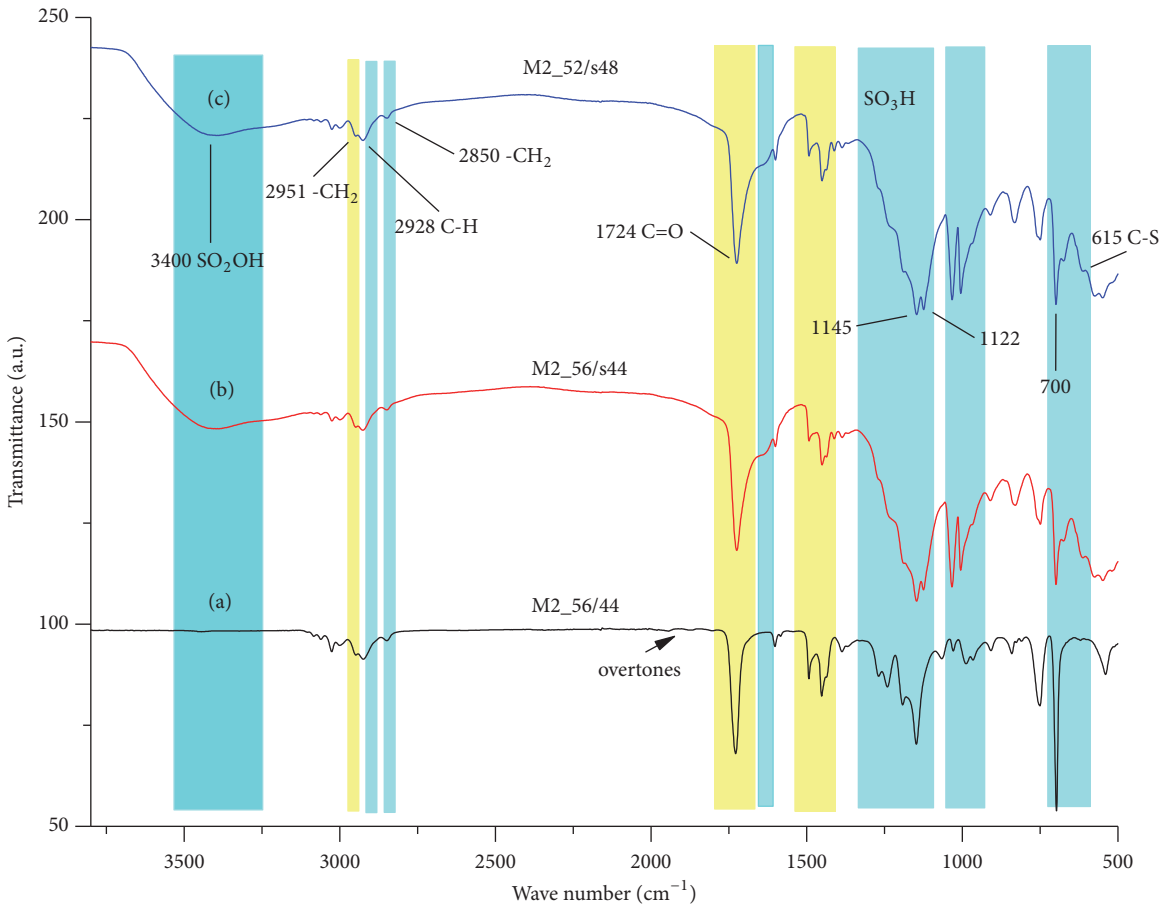

Figure 1: FT-IR spectra of (a) a nonsulfonated PMMA-*b*-PS (M2_56/44 in Table 1) and of sulfonated BCs (PMMA-*b*-sPS in Table 2): (b) M2_56/s44 (DS = 87 %) and (c) M2_52/s48 (DS = 90 %).

Table 1 also shows the calculated value of the product of the Flory-Huggins interaction parameter (χ) and the total (N). χ was calculated from (1), where T is the absolute temperature of the system [21].

$$\chi = 0.028 + \frac{(3.9 \pm 0.06)}{T} \quad (1)$$

3.2. FT-IR Characterization. The presence of sulfonic acid groups in the sulfonated BCs was investigated by FTIR. Representative FTIR spectra of the PMMA-*b*-PS BCs samples before and after sulfonation are shown in Figure 1. The bands highlighted in yellow correspond to stretching vibrations of PMMA segments, while cyan-colored bands correspond to PS. All nonsulfonated PMMA-*b*-PS BCs (for instance, M2_56/44) exhibited characteristic signals at 2930 and 2850 cm^{-1} associated with stretching vibrations of methyl and methylene groups, respectively. In addition, the weak signal between 3028 and 3080 cm^{-1} can be ascribed to the vibrations of C-H bonds in the aromatic rings. Other vibrations of monosubstituted aromatic rings also called "overtones" were observed between 1950 and 1800 cm^{-1}, while the strong band approximately observed at 700 cm^{-1} was attributed to an out-of-the-plane bending vibration of the C-H bond [22]. As compared to the nonsulfonated samples, all sulfonated BCs (see, for instance, M2_56/s44 and M2_52/s48) exhibited significant differences in the 1000-1200 cm^{-1} region associated with characteristic vibrations of the sulfonic acid groups (S=O, S-O, and O=S=O at 1031, 1123, and 1146 cm^{-1}, respectively) [23]. Additionally, there were a decrease in intensity and a split for signals around 700 and 1148 cm^{-1}, respectively, which can be ascribed to the reduction of the vibration symmetry produced by the presence of sulfonic groups. Although stretching vibrations of the C–S bonds are weak and of variable position, they could be observed between 600 and 700 cm^{-1} for all the sulfonated materials of this investigation [24]. Finally, the presence of O-H bonds attributed to the sulfonic acid groups (SO_2OH) and water absorption from the BC hydrophilic segments, evidenced by strong and broad signal appearing centered at approximately 3400 cm^{-1}, provided further evidence of the occurrence of the sulfonation reaction [25, 26].

3.3. Sulfur Content by ICP Characterization. Elemental analysis based on the ICP technique was utilized to quantify the sulfur content of the sulfonated BCs. The theoretical ion exchange capacity (IEC) in dry samples was estimated from these data as well. IEC can be related to the number of

Table 2: Sulfur content, ion-exchange capacities (IEC) and degree of sulfonation (DS) of PMMA-*b*-sPS BCs.

Polymer	Sulfur % (w/w)	IEC (mmol g^{-1})	DS (%)	w_{PMMA}
Macroinitiators	0.23-0.26	0		
M1_76/s24	1.0	0.31	17	0.756
M1_55/s45	6.3	1.9	64	0.475
M2_56/s44	8.6	2.6	87	0.461
M3_52/s48	8.9	2.7	90	0.420
M3_60/s40	4.8	1.5	53	0.636
M3_69/s31	4.9	1.3	67	0.520

protons derived from sulfonic acid groups and, theoretically, the number of protons equals the number of sites available for an ionic exchange reaction. IEC was estimated using the sulfur content as determined by elemental analysis and assuming that every sulfur atom was associated with a single sulfonic group and that all of them would be available for exchanging protons [27]. Furthermore, the DS was obtained from (2) and is defined as the ratio between the number of PS repeating units that contain an attached sulfonic acid group and the total number of PS repeating units [28].

$$\mathrm{DS}\,(\%) = \frac{(S/C)_{EA}}{(S/C)_{th}} * 100 \qquad (2)$$

where $(S/C)_{EA}$ and $(S/C)_{th}$ are the sulfur : carbon ratios obtained from elemental analysis and theoretically (assuming a full sulfonation process), respectively. Hence, IEC and DS were calculated from the sulfur content (as obtained by elemental analysis) and all these results are summarized in Table 2. It is worth mentioning that the sulfur amount contained in the PMMA-*b*-PS BCs precursors as a consequence of the RAFT synthesis was also subtracted from the total amount of sulfur experimentally determined in this investigation in order to achieve a more accurate estimation. Thus, the sulfur content of the obtained PMMA-*b*-sPS BCs varied from 1 to 8.9 wt. %.

3.4. ^{1}H-NMR Characterization. Selective sulfonation in one of the segments of BCs is highly desirable for some applications, such as proton exchange membranes. The sulfonated block can act as a hydrophilic phase during the formation of ionic domains, whereas the nonsulfonated block prevents the excess of swelling in the membranes [29]. Additionally, a high DS may increase the proton conductivity, improving therefore the performance of fuel cells [30]. DS was not obtained from ^{1}H-NMR since it may introduce some artifacts, caused by the presence of exchangeable protons, which could broad, shift, and modify the intensity of the signal of sulfonic proton. In this regard, the presence of sulfonic acid groups in the investigated PMMA-*b*-sPS BCs was determined by ^{1}H-NMR. Figure 2 displays ^{1}H-NMR spectra of a pristine PMMA-*b*-PS BC as well as of the sulfonated analogue sample. Protons at 3.64, 1.77, and 1.27 ppm in spectrum (a) corresponded to methoxy, methylene, and α-methyl groups from PMMA (c, e, and d), respectively. The signals attributed to the aromatic

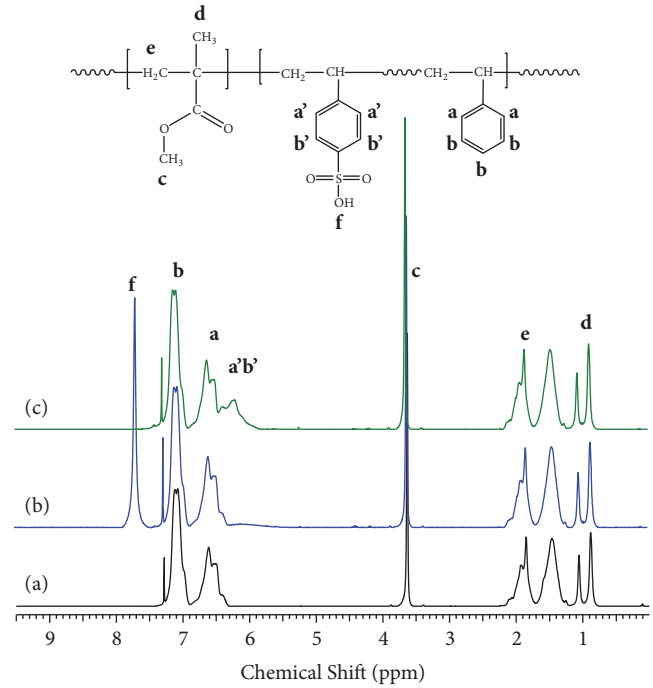

Figure 2: ^{1}H NMR spectra of PMMA-*b*-PS and PMMA-*b*-sPS BCs in $CDCl_3$ at 27°C. (a) PMMA-*b*-PS BC: M3_60/40, (b) PMMA-*b*-sPS BC: M3_60/s40. (c) PMMA-*b*-sPS BC: M3_60/s40 in a $CDCl_3/D_2O$ mixture at 27°C.

protons of PS typically appear between 6.6 and 7.1 ppm (a and b) in a pure PMMA-*b*-PS BC [25].

In the case of the sulfonated BC (PMMA-*b*-sPS), the obtained ^{1}H-NMR spectra showed some differences depending on the deuterated solvent utilized for the analysis. Sulfonic acid groups ($-SO_3H$) can form hydrogen bonds with their oxygen atom, which can affect the chemical shift (δ) and the electron density around the proton of $-SO_3H$ groups [30]. In $CDCl_3$ (spectrum b in Figure 2), the signal appearing at 7.8 ppm (f) suggested the presence of labile protons (-OH on the sulfonic acid group (-SO_3H)), which are commonly associated with N or O atoms.

The δ will mainly depend on the utilized solvent because these protons are acidic and, therefore, exchangeable. These protons typically exhibit broad singlets and usually do not couple with neighboring protons. Exchangeable protons can

Table 3: Results from the SAXS characterization.

Polymer	Morphology†	q∗ (nm^{-1})	d (nm)
M2_52/48	LAM	0.134	46.9
M2_52/s48	--	--	--
M2_56/44	LAM	0.135	46.5
M2_56/s44	--	--	--
M3_60/40	LAM	0.075∗	83.8
M3_60/s40	HPC	0.092∗	68.4

† LAM = lamellar, HPC = hexagonally packed cylinders
∗The first Bragg reflection of these samples was estimated from the higher order reflections.

be identified by ^{1}H-NMR analysis with an experiment known as "D_2O shake" [31]. If a protic-deuterated solvent is used, such as D_2O or CD_3OD (methanol-d_4), then OH protons will be exchanged with deuterium and the corresponding ^{1}H-NMR signals might shrink or entirely vanish in the spectra. Spectrum (c) in Figure 2 demonstrated this effect for one of the sulfonated BCs of this work using $CDCl_3$ solvent containing a small amount of D_2O. The signals associated with the PS aromatic ring also exhibited modifications attributed to the presence of the sulfonic acid groups. In this regard, it has been reported that the discussed sulfonation reaction mainly occurs at the *para*-position. Coughlin *et al.* associated this preferential behavior to the steric hindrance of the polymer backbone [32]; however, it could be also ascribed to the highest electron density (or highest affinity for strong electrophilic substances) observed at this position. It should be also noted that the signals attributed to the PMMA segments remain unmodified, which suggests that degradation or hydrolysis (typically reported for acrylates in presence of strong acids [33]) did not take place in this case, probably due to the utilized milder reaction conditions, *i.e.*, acetyl sulfate instead of sulfuric acid and mild reaction temperatures.

3.5. Morphology of Bulk Samples before and after Sulfonation. The equilibrium morphologies of diblock copolymers and the conditions under which they form are well known [34]. The morphology formed by a specific diblock copolymer depends on the composition as measured by the volume fraction and the degree of segregation which is determined by the product χN. Samples M2_56/44, M2_52/48, and M3_60/40 have PMMA volume fractions of 0.56, 0.52, and 0.60, respectively, and χN values above those of the order-disorder transition (see Table 1). Therefore, it is expected that these samples will form ordered morphologies. SAXS characterization (see Figure S1 in the Supplementary Materials) showed that the three samples formed lamellar morphologies (Table 3). After sulfonation, samples M2_52/s48 and M2_56/s44 did not form ordered morphologies, whereas sample M3_60/s40 formed hexagonally packed cylinder morphology. In the case of the higher molar mass sample M3_60/40 before and after sulfonation, the first Bragg reflection was estimated from higher order reflections.

When the electron charge distribution of the PS block changes by the addition of an electrophilic heteroatom, i.e., sulfur, χ will also change. χ can be estimated from the solubility parameter of polymers (δ) according to (3), where T is the absolute temperature, R is the universal gas constant, and Vc is the average molar volume of the repeating monomer units:

$$\chi_{A,B} = \frac{(\delta_A - \delta_B)^2 V_c}{RT} \quad (3)$$

Reported δ values for PMMA and PS at 298 K are 9.7 and 9.1 $(cal{\cdot}cm^{-3})^{1/2}$, respectively [35]. The reported value of δ for sPS is 16.6 $(cal{\cdot}cm^{-3})^{1/2}$ at 298 K [36], which is considerably higher than that one observed for pure PS because the intermolecular cohesive forces are different, and interactions within the sulfonated PS domains might form ionic clusters. χ will, therefore, increase after sulfonation. While mass fraction of PMMA in the BCs decreases after sulfonation (see Tables 1 and 2), the volume fraction of PMMA is likely to change also but cannot be calculated since the density of the partially sulfonated PS block is unknown. The sulfonation process will still result in block copolymers that self-assemble into an ordered morphology, but the morphology could be different from that of the starting material. SAXS characterization (see Supplementary Materials) of the sulfonated samples M2_56/s44 and M2_52/s48 did not show clear Bragg peaks, possibly because of limitations in the minimum dispersion angle that can be measured in the instrument used and poor ordering or lack of long-range order of the samples. In contrast, the SAXS results of M3_60/s40 were consistent with a morphology of hexagonally packed cylinders.

3.6. Morphological Characterization of Thin Films by Atomic Force Microscopy (AFM). As mentioned before, the final morphology of the BC is a function of χ, N, and ϕ. However, when prepared as thin films, the BCs are confined by a surface and their behavior deviates from the bulk. In thin films other parameters govern the adopted morphology and domain orientation, including interfacial interactions between the different blocks and the substrate, surface energies, and film thickness (t_o) [13, 34, 37]. In the present work, thin films of the samples before and after sulfonation with thickness near the value of the domain spacing (d) were obtained. According to Jung et al., when the thickness of the film is close to the d value, the interfacial interactions between both the substrate surface and free surface, with the BC chains, become more pronounced [38].

Thin films of samples before and after sulfonation were prepared by spin coating and characterized by AFM. Figure 3 shows the AFM images of the nonsulfonated and sulfonated (DS~50%) M3_60/40 sample, after TA at 170°C for 24 hours. TA promoted the formation of ordered morphologies since polymeric chains are provided with enough energy and mobility to reach an equilibrium configuration. For this to occur, it is necessary to heat above the glass transition temperature (T_g) of each component block in the system (PMMA T_g = 105°C, PS T_g = 100°C, and sPS T_g = 110-140°C). For the nonsulfonated BCs deposited on silicon wafers, the PMMA blocks tend to interact with the native oxide layer, preferentially wetting the surface, while PS segregates to the

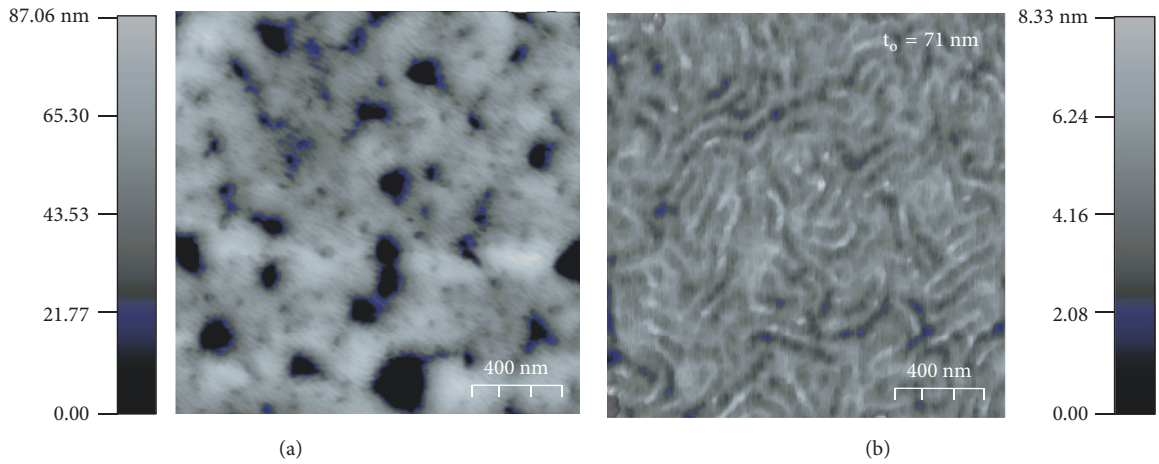

Figure 3: AFM height images of BCs thermally annealed (TA) at 170°C for 24 h. (a) M3_60/40, (b) M3_60/s40 (t_o=71 nm).

air interface due to its lower surface energy. On samples with lamellar morphology such as M2_56/44, M2_52/48, and M3_60/40, the preferential segregation induces the parallel orientation of both blocks and hence formation of layers that are observed in AFM images by the presence of islands and holes on the top surface of the film. Figure 3(a) shows an AFM image of the surface of a thin film prepared from M3_60/40. The depth of the holes observed in Figure 3(a) (87 nm) is similar to the lamellar spacing of the sample (83.8 nm) which is consistent with lamellae aligned parallel to the surface. In contrast, thin films of the same sample after sulfonation (M3_60/s40) exhibited a clear phase separation with a fingerprint type motif (Figure 3(b)). This is consistent with lamellae aligned perpendicular to the surface or cylinders aligned parallel to the surface. The latter is also consistent with the bulk morphology found for this sample by SAXS (Table 3). Changes in domain orientation upon sulfonation may be caused by the balance between the different surface energies and the interactions of the sulfonic groups with silicon oxide on the substrate surface. A perpendicular orientation of the morphology is highly desirable in applications such as templates for nanomanufacturing. This domain orientation has been obtained by employing such methodologies as deposition of a polymer brush anchored to the substrate surface to attain a neutral surface and by photolithographic techniques, among others [13, 39].

Figure 4 shows the AFM images of highly sulfonated samples (M2_56/s44 DS of 87% and M2_52/s48 DS of 90%) without any annealing treatment. Both samples formed a honeycomb-like morphology, where the domains formed were relatively larger in the sample M2_52/s48 (Figure 4(b)). This morphology may be the result of the formation of micellar aggregates in the polymer solution (polymer concentration of 0.5 w/w%, in a mixture of toluene/dioxane 50/50 v/v) and the subsequent arrangement of the micelles during the rapid evaporation of the solvent. The polymer solution exhibited a slightly turbid appearance and high stability since the polymer remained well dispersed with time. According to Nehache et al., this type of morphology is obtained in solution rather than by self-assembly of the BC in solid state, while the formation of the honeycomb structure and the pore size depend on the evaporation rate and concentration of the pair of solvents employed for dissolving the BC [10]. In the present work, the concentration of the solvents was the same for the samples presented in Figure 4. Thus, slight variations in the DS may cause large differences in the size of the domains. As mentioned before in Section 3.2, FTIR spectra showed the water absorption of the highly sulfonated bulk samples. Thus, it is not discarded that thin films may undergo water uptake due to the hydrophilic nature of the sulfonated segments, hence also contributing to swelling of these domains and influencing the obtained morphology. However, this is unlikely since the films samples were dried under vacuum before the AFM analysis.

Figure 5 shows AFM images of thin films of M2_52/s48, the BC with the highest DS (90 %), after being subjected to different treatments including TA and SVA. Figure 5(a) shows the morphology of the sample treated at 170°C for 24 h. The AFM image clearly shows phase separation, but the domains do not assemble into an ordered morphology. However, the domain arrangement is bicontinuous which could be indicative of a gyroid morphology. Figure 5(b) shows the corresponding morphology of the sample subjected to the SVA treatment with THF solvent. Based on the solubility parameter of PMMA, sPS, and THF, with values of 9.7, 16.6, and 9.84 $(\text{cal}\cdot\text{cm}^{-3})^{1/2}$, respectively, THF could preferentially swell PMMA instead of the sulfonated PS segment. As a result, the observed morphology was a micelle-like structure obtained at room temperature after 3 hours of exposition to the solvent. Yang and Loos obtained micelle-like structures in thin films of PS-b-P2VP copolymers exposed to toluene vapor [9]. They concluded that the use of a selective solvent might result in nonequilibrium morphologies such as the micelle-like structure, rather than one of the equilibrium morphologies. Figure 5(c) shows the morphology of the sample exposed to dioxane at room temperature for 3 hours. This is a good solvent for the sulphonated PS segment and a poor solvent for the PMMA and PS blocks. The resulting

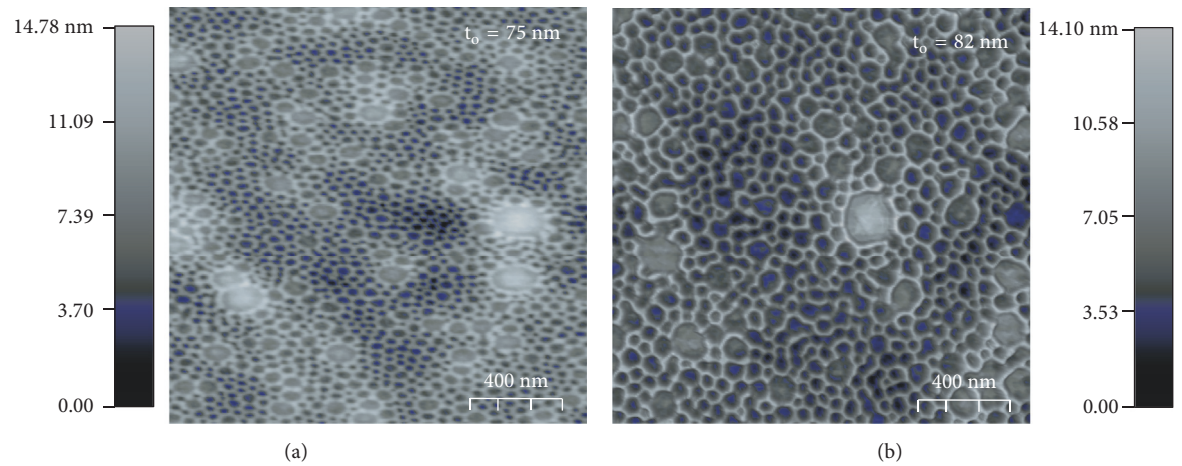

Figure 4: AFM height images of highly sulfonated samples without any annealing treatment. (a) M2_52/s48 DS of 90% and (b) M2_56/s44 DS of 87%.

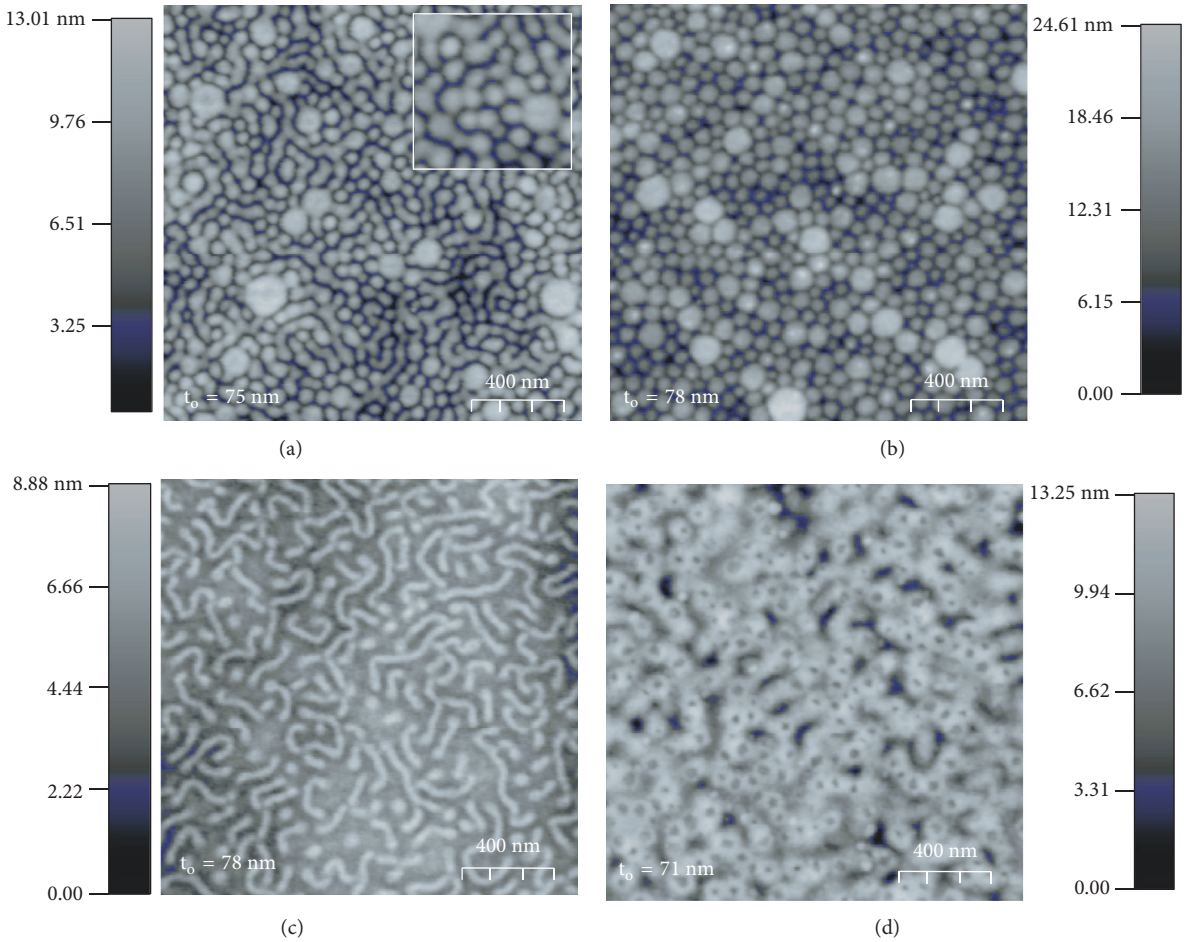

Figure 5: AFM height images of a highly sulfonated BC (M2_52/s48) subjected to different annealing treatments. (a) Thermally annealed (TA) at 170°C for 24 h. (b) SVA treated with THF (3 h), (c) SVA treated in a mixture of toluene/dioxane (50/50 v/v % for 3h). (d) SVA treated with dioxane for 3 h.

morphology was a worm-like structure. According to Zhao et al., this type of morphology is produced by the opposite movement of the blocks caused by the swelling of the sPS block and the contraction of the other block [8]. Figure 5(d) shows the morphology of sample acquired after the exposing a film to a mixture of toluene/dioxane (50/50 v/v%). The mixture of polar and nonpolar solvents interacts with both the sPS and PMMA domains. The obtained morphology is a mixture of worm-like and spherical micelle-like structures. This type of morphology was obtained because of chain extension configuration at different swelling and deswelling rates.

As reported in other works, the final equilibrium or nonequilibrium morphology obtained greatly depends on several variables such as the TA conditions, the solvent, concentration, and time and exposure temperature for the SVA treatment [9, 40]. Specifically, for the system reported herein (PMMA-*b*-sPS), the introduction of sulfonic acid groups greatly modifies the chemical interactions between the polymer chains and the solvents, resulting in different equilibrium and nonequilibrium (micelle and worm-like) morphologies. In addition to obtaining several morphologies, the sulfonic groups introduced ionically conductive domains that may be employed as polyelectrolytes in the bulk state and also in the form of thin films for covering and binding catalytic particles, providing conductive pathways for ions and reactant species in fuel cell applications.

4. Conclusions

In the present work sulfonated block copolymers based on PMMA-*b*-PS were prepared and characterized chemically and structurally by FT-IR, ^{1}HNMR, elemental analysis, and AFM. The selective sulfonation of PS segments in the PMMA-*b*-PS BC system is highly desirable in some applications where the formation of ionic conductive pathways at the nanoscale level is desired. The thin films showed lamellar or cylinder equilibrium morphologies for a medium DS, while the high DS films showed a honeycomb morphology, where the domains size decreased with increasing DS. The TA and solvent vapor exposure (SVA) treatments modified the resulting structure, observing a variety of equilibrium and nonequilibrium morphologies such as a bicontinuous structure, micelles, worm-like, and a combination of worm-like and micelles structures. The honeycomb-like structure was obtained due to the formation of micellar aggregates in solution rather than by self-assembly in solid state. The nonequilibrium morphologies were produced by the different swelling and deswelling ratios of the blocks exposed to selective solvents. In fuel cell applications these nanostructured thin films may be employed for covering and binding catalytic particles, providing conductive pathways for ions and reactant species.

Data Availability

All the data used in this work has been provided in the text and in the supplementary materials. Any request could be directed to the corresponding authors email: jose.bonilla@cimav.edu.mx, or carlos.guerrero.sanchez@uni-jena.de.

Conflicts of Interest

The authors declare that there is not conflict of interest regarding the publication of this paper.

Acknowledgments

Claudia Piñón-Balderrama and José Bonilla-Cruz thank the Consejo Nacional de Ciencia y Tecnología (CONACyT, México) for the doctoral scholarship and supporting this research (grant no. 182631-2012). The authors also thank Dr. Oscar Vega and M.S. Oscar Solís for the acquisition of AFM images. Carlos Guerrero-Sanchez and Ulrich S. Schubert thank CONACyT and the Deutscher Akademischer Austauschdienst (DAAD, Germany) for financial support within the framework of the funding program for international mobility PROALMEX 2015 (CONACyT project: 267752 and DAAD project: 57271725) as well as the Collaborative Research Center "PolyTarget" (SFB 1278, projects B02 and Z01) of the Deutsche Forschungsgemeinschaft (DFG, Germany) for financial support.

Supplementary Materials

SAXS analysis used to support the findings of this study is included within the supplementary materials file as Figure S1: SAXS results for bulk samples a) M2_52/48, b) M2_52/s48, c) M2_56/44, d) M2_56/s44, e) M3_60/40, and f) M3_60/s40. *(Supplementary Materials)*

References

[1] Y. Fink, A. M. Urbas, M. G. Bawendi, J. D. Joannopoulos, and E. L. Thomas, "Block copolymers as photonic bandgap materials," *Journal of Lightwave Technology*, vol. 17, no. 11, pp. 1963–1969, 1999.

[2] Q.-Y. Tang and Y.-Q. Ma, "High density multiplication of graphoepitaxy directed block copolymer assembly on two-dimensional lattice template," *Soft Matter*, vol. 6, no. 18, pp. 4460–4465, 2010.

[3] M. Park, C. Harrison, P. M. Chaikin, R. A. Register, and D. H. Adamson, "Block copolymer lithography: periodic arrays of ~ 10^{11} holes in 1 square centimeter," *Science*, vol. 276, no. 5317, pp. 1401–1404, 1997.

[4] T. Thurn-Albrecht, J. Schotter, G. A. Kastle et al., "Ultrahigh-density nanowire arrays grown in self-assembled diblock copolymer templates," *Science*, vol. 290, no. 5499, pp. 2126–2129, 2000.

[5] C. Sinturel, M. Vayer, M. Morris, and M. A. Hillmyer, "Solvent vapor annealing of block polymer thin films," *Macromolecules* , vol. 46, no. 14, pp. 5399–5415, 2013.

[6] Y. Zhao, "Structural changes upon annealing in a deformed styrene-butadiene-styrene triblock copolymer as revealed by infrared dichroism," *Macromolecules*, vol. 25, no. 18, pp. 4705–4711, 1992.

[7] K. Amundson, E. Helfand, D. D. Davis, X. Quan, S. S. Patel, and S. D. Smith, "Effect of an electric field on block copolymer microstructure," *Macromolecules*, vol. 24, no. 24, pp. 6546–6548, 1991.

[8] B. Zhao, W. J. Brittain, W. Zhou, and S. Z. D. Cheng, "Nanopattern formation from tethered PS-b-PMMA brushes upon treatment with selective solvents," *Journal of the American Chemical Society*, vol. 122, no. 10, pp. 2407-2408, 2000.

[9] Q. Yang and K. Loos, "Perpendicular structure formation of block copolymer thin films during thermal solvent vapor annealing: solvent and thickness effects," *Polymer*, vol. 9, no. 10, p. 525, 2017.

[10] S. Nehache, M. Semsarilar, M. In et al., "Self-assembly of PS-PNaSS-PS triblock copolymers from solution to the solid state," *Polymer Chemistry*, vol. 8, no. 21, pp. 3357–3363, 2017.

[11] T. P. Russell, R. P. Hjelm, and P. A. Seeger, "Temperature Dependence of the Interaction Parameter of Polystyrene and Poly(methyl methacrylate)," *Macromolecules* , vol. 23, no. 3, pp. 890–893, 1990.

[12] S. H. Anastasiadis, T. P. Russell, S. K. Satija, and C. F. Majkrzak, "Neutron reflectivity studies of the surface-induced ordering of diblock copolymer films," *Physical Review Letters*, vol. 62, no. 16, pp. 1852–1855, 1989.

[13] P. Mansky, Y. Liu, E. Huang, T. P. Russell, and C. Hawker, "Controlling polymer-surface interactions with random copolymer brushes," *Science*, vol. 275, no. 5305, pp. 1458–1460, 1997.

[14] T. Xu, A. V. Zvelindovsky, G. J. A. Sevink, K. S. Lyakhova, H. Jinnai, and T. P. Russell, "Electric field alignment of asymmetric diblock copolymer thin films," *Macromolecules* , vol. 38, no. 26, pp. 10788–10798, 2005.

[15] L. Rubatat, C. Li, H. Dietsch, A. Nykänen, J. Ruokolainen, and R. Mezzenga, "Structure-properties relationship in proton conductive sulfonated polystyrene-polymethyl methacrylate block copolymers (sPS-PMMA)," *Macromolecules* , vol. 41, no. 21, pp. 8130–8137, 2008.

[16] T. Erdogan, E. E. Unveren, T. Y. Inan, and B. Birkan, "Well-defined block copolymer ionomers and their blend membranes for proton exchange membrane fuel cell," *Journal of Membrane Science*, vol. 344, no. 1-2, pp. 172–181, 2009.

[17] R. A. Weiss, A. Sen, C. L. Willis, and L. A. Pottick, "Block copolymer ionomers: 1. Synthesis and physical properties of sulphonated poly(styrene-ethylene/butylene-styrene)," *Polymer Journal*, vol. 32, no. 10, pp. 1867–1874, 1991.

[18] J. Bonilla-Cruz, C. Guerrero-Sánchez, U. S. Schubert, and E. Saldívar-Guerra, "Controlled "grafting-from" of poly[styrene-co-maleic anhydride] onto polydienes using nitroxide chemistry," *European Polymer Journal*, vol. 46, no. 2, pp. 298–312, 2010.

[19] M. B. Smith and J. March, *March's Advanced Organic Chemistry: Reactions, Mechanisms, and Structure*, John Wiley & Sons, 2007.

[20] F. Kučera and J. Jančář, "Homogeneous and heterogeneous sulfonation of polymers: a review," *Polymer Engineering & Science*, vol. 38, no. 5, pp. 783–792, 1998.

[21] T. P. Russell, R. P. Hjelm, and P. A. Seeger, "Temperature dependence of the interaction parameter of polystyrene and poly(methyl methacrylate)," *Macromolecules*, vol. 23, no. 3, pp. 890–893, 1990.

[22] M. Hatamzadeh and M. Jaymand, "Synthesis and characterization of polystyrene-graft-polythiophene via a combination of atom transfer radical polymerization and Grignard reaction," *RSC Advances*, vol. 4, no. 32, pp. 16792–16802, 2014.

[23] J. W. Mays, "Synthesis of model branched polyelectrolytes," *Polymer Communications Guildford*, vol. 31, no. 5, pp. 170-171, 1990.

[24] J. C. Yang, M. J. Jablonsky, and J. W. Mays, "NMR and FT-IR studies of sulfonated styrene-based homopolymers and copolymers," *Polymer Journal*, vol. 43, no. 19, pp. 5125–5132, 2002.

[25] W. Wang, H. Zhang, W. Geng et al., "Synthesis of poly (methyl methacrylate)-b-polystyrene with high molecular weight by DPE seeded emulsion polymerization and its application in proton exchange membrane," *Journal of Colloid and Interface Science*, vol. 406, pp. 154–164, 2013.

[26] R. M. Silverstein, F. X. Webster, D. J. Kiemle, and D. L. Bryce, *Spectrometric Identification of Organic Compounds*, John wiley & Sons, 2014.

[27] P. Bébin, M. Caravanier, and H. Galiano, "Nafion/clay-SO_3H membrane for proton exchange membrane fuel cell application," *Journal of Membrane Science*, vol. 278, no. 1-2, pp. 35–42, 2006.

[28] H.-C. Lee, H. Lim, W.-F. Su, and C.-Y. Chao, "Novel sulfonated block copolymer containing pendant alkylsulfonic acids: Syntheses, unique morphologies, and applications in proton exchange membrane," *Journal of Polymer Science Part A: Polymer Chemistry*, vol. 49, no. 11, pp. 2325–2338, 2011.

[29] T. Higashihara, K. Matsumoto, and M. Ueda, "Sulfonated aromatic hydrocarbon polymers as proton exchange membranes for fuel cells," *Polymer Journal*, vol. 50, no. 23, pp. 5341–5357, 2009.

[30] S. Mulijani, K. Dahlan, and A. Wulanawati, "Sulfonated polystyrene copolymer: synthesis, characterization and its application of membrane for direct methanol Fuel Cell (DMFC)," *International Journal of Materials, Mechanics and Manufacturing*, vol. 2, pp. 36–40, 2014.

[31] D. L. Pavia, G. M. Lampman, G. S. Kriz, and J. A. Vyvyan, "Introduction to spectroscopy," *Cengage Learning*, 2008.

[32] J. E. Coughlin, A. Reisch, M. Z. Markarian, and J. B. Schlenoff, "Sulfonation of polystyrene: Toward the "ideal" polyelectrolyte," *Journal of Polymer Science Part A: Polymer Chemistry*, vol. 51, no. 11, pp. 2416–2424, 2013.

[33] J. Semen and J. B. Lando, "The Acid Hydrolysis of Isotactic and Syndiotactic Poly (methyl methacrylate)," *Macromolecules* , vol. 2, no. 6, pp. 570–575, 1969.

[34] R. Olayo-Valles, S. Guo, M. S. Lund, C. Leighton, and M. A. Hillmyer, "Perpendicular domain orientation in thin films of polystyrene-polylactide diblock copolymers," *Macromolecules*, vol. 38, no. 24, pp. 10101–10108, 2005.

[35] M. M. Coleman, C. J. Serman, D. E. Bhagwagar, and P. C. Painter, "A practical guide to polymer miscibility," *Polymer Journal*, vol. 31, no. 7, pp. 1187–1203, 1990.

[36] D. W. Van Krevelen and K. Te Nijenhuis, *Properties of Polymers: Their Correlation with Chemical Structure; Their Numerical Estimation and Prediction from Additive Group Contributions*, Elsevier, 2009.

[37] D. Y. Ryu, S. Ham, E. Kim, U. Jeong, C. J. Hawker, and T. P. Russell, "Cylindrical microdomain orientation of PS-b-PMMA on the balanced interfacial interactions: composition effect of block copolymers," *Macromolecules*, vol. 42, no. 13, pp. 4902–4906, 2009.

[38] J. Jung, H.-W. Park, S. Lee et al., "Effect of film thickness on the phase behaviors of diblock copolymer thin film," *ACS Nano*, vol. 4, no. 6, pp. 3109–3116, 2010.

[39] Q. J. Niu and J. M. J. Fréchet, "Polymers for 193-nm microlithography: Regioregular 2-alkoxycarbonylnortricyclene polymers by controlled cyclopolymerization of bulky ester derivatives of norbornadiene," *Angewandte Chemie International Edition*, vol. 37, no. 5, pp. 667–670, 1998.

[40] M. J. Fasolka and A. M. Mayes, "Block copolymer thin films: Physics and applications," *Annual Review of Materials Research*, vol. 31, no. 1, pp. 323–355, 2001.


The Scientific
World Journal
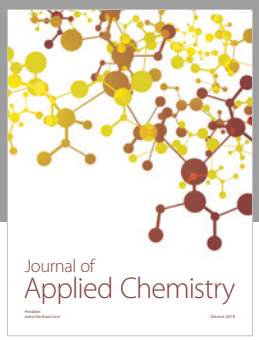
Journal of
Applied Chemistry
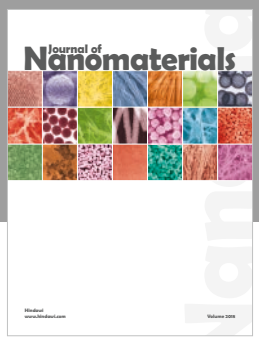
Journal of
Nanomaterials

Scientifica

International Journal of
Polymer Science
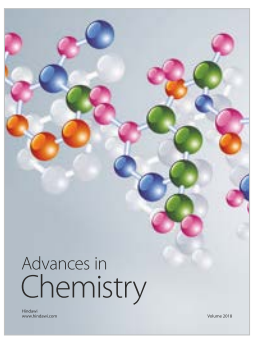
Advances in
Chemistry

Hindawi
Submit your manuscripts at
www.hindawi.com
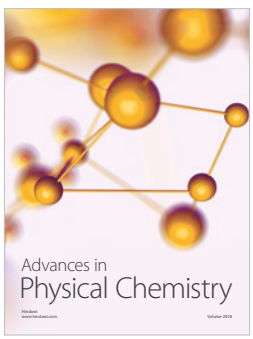
Advances in
Physical Chemistry

International Journal of
Analytical Chemistry
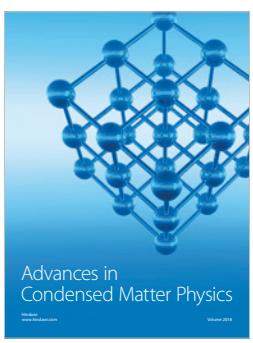
Advances in
Condensed Matter Physics
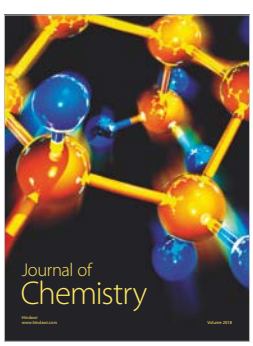
Journal of
Chemistry

International Journal of
Biomaterials
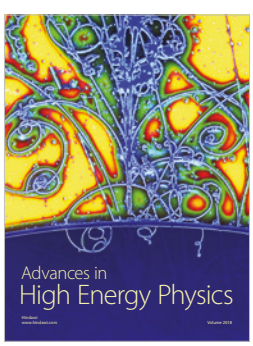
Advances in
High Energy Physics

Journal of
Engineering

Journal of
Nanotechnology

International Journal of
Corrosion

Journal of
Materials

BioMed
Research International
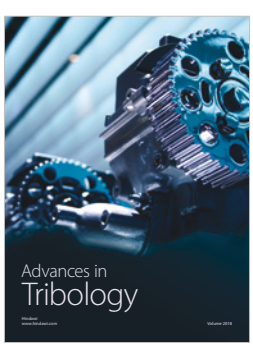
Advances in
Tribology
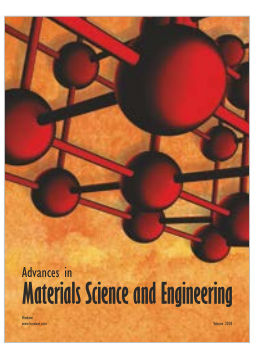
Advances in
Materials Science and Engineering